AMERICAN SOCIETY of
GENE & CELL
THERAPY

Tween 85-Modified Low Molecular Weight PEI Enhances Exon-Skipping of Antisense Morpholino Oligomer In Vitro and in *mdx* Mice

Mingxing Wang,[1] Bo Wu,[1] Jason D. Tucker,[1] Sapana N. Shah,[1] Peijuan Lu,[1] Lauren E. Bollinger,[1] and Qilong Lu[1]

[1]McColl-Lockwood Laboratory for Muscular Dystrophy Research, Carolinas Medical Center, 1000 Blythe Blvd., Charlotte, NC 28231, USA

We investigated a series of Tween 85 modified low molecular weight polyethylenimine (LPEI, 0.8k/1.2k/2.0k)-copolymers (Zs) through simple formulation and covalent conjugation with phosphorodiamidate morpholino oligomer (PMO) for their potential to enhance delivery in vitro and in dystrophic *mdx* mice. Z polymers significantly enhanced PMO-induced exon-skipping in a GFP reporter-based cell culture system. Application of optimized formulations of Zs with PMO targeted to dystrophin exon 23 demonstrated a significant increase in exon-skipping efficiency in *mdx* mice. Consistent with our observations in vitro, optimization of molecular size and hydropholic-lipopholic balance (HLB) of polymers are important factors to achieve enhanced PMO delivery in vivo. The best formulation of Zs enhanced PMO delivery with 20- and 6-fold over PMO alone in vitro and in vivo, respectively. Further, chemical conjugation of the polymer and PMO exhibits greater benefit than polymer/PMO simple formulation in PMO delivery efficiency. Observed cytotoxicity of the Zs was lower than Endo-porter and PEI 25k in vitro, and no tissue toxicity was clearly detected with the Zs at the dosage tested. These results indicate the potential of the Zs as effective and safe PMO delivery carriers for treating diseases such as muscular dystrophy.

INTRODUCTION

Duchenne muscular dystrophy (DMD) is a fatal muscle disorder caused by nonsense or frameshift mutations in the dystrophin gene affecting approximately 1 in 5,000 male births.[1–4] Fundamental treatments of DMD requires either correction or replacement of the mutated gene to restore function. The large size of dystrophin protein and the requirement of lifetime administration to muscles throughout the body severely limit the progress in developing effective experimental therapies.[5] In recent years, antisense oligonucleotide (AO)-mediated exon-skipping has been a promising therapy for treating DMD by facilitating "skipping" of specific dystrophin gene exon(s) to restore the open reading frame for the dystrophin mRNA.[6–18] Currently, phosphorodiamidate morpholino oligomers (PMOs) have been widely studied in exon-skipping therapy for DMD and applied in clinical trials,[10–13] as well as have recently resulted in FDA approval for exondys 51 (see review).[19,20] PMO is an uncharged oligonucleotide, which has better stability and less toxicity compared

with other chemically modified AOs. However the uncharged nature of naked PMO relies on passive diffusion to enter cells, thus less effective for in vivo delivery.[15,21] To increase delivery efficiency, cell penetrating peptides and cationic dendrimer have been chemically conjugated to PMO, and substantial improvement in delivery has been reported in *mdx* mice in vivo, resulting in near-normal levels of dystrophin expression in body-wide muscles.[9,14–16] However, the densely packed and highly positive-charged peptides are associated with higher toxicity with an LD50 near 100 mg/kg, making clinical applications challenging.[16] In addition, the complicated synthesis and purification in covalent modification make it more expensive, and potential peptide-related immune responses could prevent repeated administration. Recently, some small molecules have been demonstrated to promote uptake of AOs in *mdx* mice with enhanced exon-skipping. These include Dantrolene-aided PMO delivery studied by Kendall et al.,[22] and monosaacharide-formulated AOs reported by Yin's group.[23,24] Polymer-based non-viral delivery remains attractive, because of the polymer's structural flexibilities (including different molecular size, hydrophilic-lipophilic balance, and charge density), extensive resources from synthetic or natural, larger capacity for therapeutic agents, low host immunogenicity, and with relatively low expense.[25]

Amphiphilic polymers have been developed for gene delivery by our group and others, demonstrating enhanced gene transfection in skeletal muscles.[26–35] Recently, a series of cationic amphiphilic Z polymers constructed from Tween 85 (T85) and low molecular weight (Mw) polyethyleneimine (LPEI) were prepared and characterized for pDNA and antisense 2′-O-methyl-phosphorothioate RNA (2′-OMePS) delivery in vitro and in vivo,[33,34] which can condense pDNA/2′-OMePS efficiently with nanosize particles below 200 nm at the weight ratio 5 of polymer/pDNA or 2′-OMePS, being stable in the presence of serum glycosaminoglycans (GAGs) and heparin. The introduction of T85 led to a significant increase in the cellular

CrossMark

Table 1. Characteristics of T85-LPEI (Z polymers)

| Code | Composition (Molar Ratio)[a] | N (%)[b] | Mw (Da) | | PEI (%)[d] | Grafted T85 /PEI[b] |
			EA[b]	^{1}H NMR[c]		
Z0	T85	0			0	
Z1	T85-PEI 0.8k (1:1)	4.43	6,019.6	6,981.4	13.28	6.53
Z2	T85-PEI 0.8k (1:3)	5.20	5,123.5	5,534.8	15.61	5.40
Z3	T85-PEI 0.8k (3:1)	4.12	6,422.5	7,223.6	12.46	7.02
Z4	T85-PEI 1.2k (1:1)	5.17	7,766.7	8,370.2	15.45	5.47
Z5	T85-PEI 1.2k (1:3)	6.24	6,410.3	5,796.3	18.72	4.34
Z6	T85-PEI 1.2k (3:1)	4.65	8,602.2	9,289.4	13.95	6.17
Z7	T85-PEI 2.0k (1:1)	2.85	23,391.8	25,863.7	8.55	10.70
Z8	T85-PEI 2.0k (1:3)	6.97	9,564.8	10,808.3	20.91	3.78
Z9	T85-PEI 2.0k (3:1)	2.75	24,242.5	29,485.6	8.25	11.12
Z8-PMO[e]	conjugate	about three PMOs were grafted onto one Z8 polymer				

[a]Feed ratio of starting materials
[b]Microanalysis of nitrogen
[c]^{1}H-NMR analysis with 500 MHz Jeol
[d]Assume the N (%) is 33.33 WT% in each PEI
[e]PMO covalent to polymer chemically

uptake of the pDNA or 2′-OMePS/polymer complexes with higher transfection efficiency (TE) in CHO, C2C12, and HSkM cell lines, but without increase in toxicity compared with the parent LPEI. The optimal polymer-formulated pDNA and 2′-OMePS produced transgene expression efficiency 15, 10-fold of pDNA and 2′-OMePS alone in *mdx* mice in vivo, respectively.

Driven by the promising performances in the delivery of pDNA and 2′-OMePS, we herein investigated the Z polymers for PMO delivery through simple formulation and covalent conjugation in vitro and in dystrophic *mdx* mice. The results indicated that (1) Z polymers improved PMO-induced exon-skipping efficiency relative to PEI 25k or Endo-porter (a commercially available reagent for PMO delivery) in vitro; (2) Z polymers in formulation significantly promoted dystrophin expression with PMO targeting the mutated mouse dystrophin exon 23 when administered both locally and systemically in *mdx* mice; (3) The Z-PMO conjugates showed more effective than corresponding Z/PMO simple formulation in terms of improved bio-distribution and delivery efficiency upon systemic delivery. Overall, enhanced exon-skipping and low toxicity potentiate Z polymers as antisense PMO delivery vector for the treatment of DMD or other genetic diseases.

RESULTS AND DISCUSSION
Synthesis and Characterization of T85-LPEI (Z) Copolymer, and Corresponding Z-PMO Conjugate
The synthesis and characterization of Z polymers have been reported in our previous study.[33] In brief, Z polymers were synthesized from T85 activated by 1,1′-carbonyldiimidazole (CDI), followed by reaction with excess LPEI (0.8k/1.2k/2.0k) with varied feed ratios.

To assess whether the chemical conjugation of polymer-PMO could alter the delivery performance of PMO compared with simple delivery formulation, we selected Z8, which has free amino groups, to conjugate with PMO. Ideally, oligonucleotide delivery systems should be stable in the bloodstream so that they can circulate long enough to allow oligonucleotides to be taken up by targeted tissues. On the other hand, to produce pharmacological function, the therapeutic oligonucleotides must be released from the delivery system in the target cells in order that they can more easily cross nuclear membrane and bind their target pre-mRNA in the nucleus.[36] We therefore utilized a bioreducible disulfide linkage to bond PMOs with polymer (Polymer-S-S-PMO), which can be potentially broken under the reducing intracellular environment, with the PMO cargo being released well within the target cells or tissue. The procedure for Z8-PMO conjugation was reported previously with some modification (see Supplemental Information).[37] The nomenclature and characteristics of the Z polymers and Z8-PMO conjugate are presented in Table 1.

Z Polymer-Mediated PMO Delivery In Vitro
The cytotoxicity of Z polymers in C2C12E50 cells was evaluated by an MTS [3-(4,5-dimethylthiazol-2-yl)-5-(3-carboxymethoxyphenyl)-2-(4-sulfophenyl)-2H-tetrazolium]-based assay, as reported previously.[34] All Zs at a dose of 20 μg/mL maintained live cells over 75%, except for Z8 (67%), which was close to LPEI. This viability was much higher than PEI 25k at 4 μg/mL. The relatively higher toxicity of Z5 and Z8 compared to other Zs likely resulted from the higher content of PEI within the polymers. The data demonstrated that the toxicity of the T85-modified LPEI does not increase with the increasing molecular size. This was partly due to fact that the primary and/or secondary amines of PEI were substituted with the cyto-biocompatible T85.

For assessing PMO delivery in vitro, the C2C12E50 myoblasts and differentiated C2C12E23 cells expressing the reporter GFP were used. The expression of GFP in the cells is disrupted by the insertion of the human dystrophin exon 50 (hDyse50) or mouse dystrophin exon 23 (mDysE23) within the GFP coding sequence. Restoration of GFP expression relied on the targeted removal of the inserted exon by AOs.[38,39]

Delivery in C2C12E50 Myoblast Cell

C2C12E50 cells were treated with 5 μg PMOE50 (5′-AACTT CCTCTTTAACAGAAAAGCATAC-3′) formulated with each polymer at two doses (5 and 10 μg) in 0.5 mL 10% fetal bovine serum (FBS)-DMEM, and the TE was determined by fluorescence microscopy and flow cytometry after 4-day treatment. TE (% of cells with GFP expression) of PMOE50 was over 70% with polymer Z3/Z4/Z5/Z6/Z7/Z9 formulated at a dose of 10 μg, comparable to or higher than Endo-porter (an effective reagent for PMO delivery in vitro developed by Gene Tools)-formulated delivery. The highest TEs were achieved with polymer Z3/Z4/Z7/Z9 reaching close to 80% and approximately 20-fold over PMO alone (around 4%) and more than 2.5 times higher than PEI 25k-formulated PMO, which produced TE of around 30% at the dose of 5 μg (PEI 25k at 10 μg killed almost all cells, as shown in our previous study). In addition, the PMO formulated with individual polymer ingredients (T85 or LPEI [PEI 0.8k, 1.2k, 2.0k]) produced very low TE (<7%) even at the dose of 10 μg. These results therefore indicate a synergy between T85 and LPEI via chemical conjugation. Concordant with the polymer alone, cytotoxicity of the amphiphilic Zs-formulated PMO at this dose remained low, with more than 75% of cells being alive for all Zs except for Z5 and Z8, which had slightly lower viability.[33,34] Again, PEI 25k or Endo-porter caused 72% or 35% cell mortality at a dose of 5 μg, respectively (Figure 1). The relationship between the polymer composition and PMO delivery efficiency is rather complicated: either polymers with moderate size and higher PEI content or large molecular size are associated with higher TE. The Z3, Z4, and Z6 with moderate size (7,200–9,300 Da) improved the delivery of size-matched PMO (around 8,000 Da) probably through polymer/PMO complex particles formed by chain-chain packing with dispersed positive surface, whereas the large-size Z7 or Z9 (over 25,000 Da) might complex PMO more flexibly and make the particles more hydrophobic to improve cell uptake.

Delivery in C2C12E23 Differentiated Cell

To evaluate the delivery potential of the Zs for PMO exon-skipping in muscle fibers, the Zs were further tested in the reporter C2C12 cell expressing mouse dystrophin exon 23 inserted into the GFP coding sequence (C2C12E23). The expression construct uses a muscle creatine kinase (MCK) promoter to drive the reporter GFP expression, thereby allowing a more cell-type-specific assessment of the potential of the Zs for PMO delivery in differentiating or differentiated myotubes.[39] Cells reaching around 70% confluence were incubated in 10% FBS media for 2 days and then treated with Zs-formulated PMOE23 or Z8-PMOE23 conjugate. The PMOE23 (5′-GGCCAAA

CCTCGGCTTACCTGAAAT-3′) targeting the boundary sequences of the inserted exon and intron 23 was used (Gene Tools). We examined Z8-PMOE23 conjugate (5 μg) and PMOE23 (5 μg) formulated with each polymer at two doses (5 and 10 μg) in 0.5 mL 10% FBS-DMEM medium, and the TE was visualized by fluorescence microscopy after 6-day treatment. The results showed that the Z8-PMO conjugate and all Z-formulated PMOs enhanced exon-skipping as compared to PMO alone. The efficacy to differentiated cells was observed, and no toxicity was detected under the tested doses as illustrated by fluorescence images, and the exon-skipping was further confirmed via RT-PCR (Figure 2). The levels of exon 23 skipping were 54.1%, 42.3%, 55.2%, 46.3%, 40.3%, 38.8%, 51.8%, 42.4%, 53.8%, 67.5%, and 12.7% for Z1-, Z2-, Z3-, Z4-, Z5-, Z6-, Z7-, Z8-, and Z9 (10 μg)-formulated PMO (5 μg), Z8-PMO (5 μg), and PMO (5 μg) only, respectively. The results, together with the consideration in the variation of molecular size, the chemical structure, and the positive charge distribution in vector microstructure, further support the hypothesis that moderate-size molecules with higher PEI content or large-size molecules are better candidates as PMO delivery carriers in C2C12E23 differentiated myotubes. Furthermore, the Z8-PMO conjugate produced a higher exon-skipping effect than the conventional polymer/PMO complex, likely due to the homogeneity of particles, less cytotoxicity, and higher drug-loading efficiency.

Our previous study showed that Z4 and Z5 have lower efficiency for pDNA and 2′-OMePS delivery in cell culture and in vivo delivery.[33,34] However, the same Zs were highly effective for PMO delivery with enhanced exon-skipping. The reasons for such an apparent difference in Z-mediated delivery for pDNA, 2′-OMePS, and PMO are as yet unclear, but the differences in chemical nature and molecular size among these three unique therapeutic cargos are primary contributors. The pDNA and 2′-OMePS are negatively charged, whereas the PMO is charge neutral. The negatively charged pDNA or 2′-OMePS requires more positively charged polymeric vector to neutralize and condense for effective delivery; the pDNA is much larger than 2′-OMePS, leading to the particle size of the polymer/cargo polyplex and the surface charge under same weight ratio of the same target and polymer to be vastly different. In contrast, Z polymer and PMO may form a complex through primarily hydrophobic interaction, and a high-order superstructure may assemble. This is supported by the fact that relatively hydrophobic polymers, such as the Z1/Z3, Z4/Z6, and Z7/Z9, enhanced PMO delivery more effectively than those relatively hydrophilic ones, such as Z2, Z5, and Z8, respectively, in each subgroup, which means the lipophilic interaction between amphiphilic polymer and uncharged PMO might therefore be one of the critical factors to enhance PMO delivery. In addition, positively charged groups within the Zs are likely not crucial for interaction with PMO, but they could afford the polyplex particles in a biological environment a longer circulation time than naked PMO. This may well lead to a higher serum tolerance and improvement in the uptake of PMO from the vasculature and across the cell membrane, therefore resulting in more effective delivery of PMO into muscles.
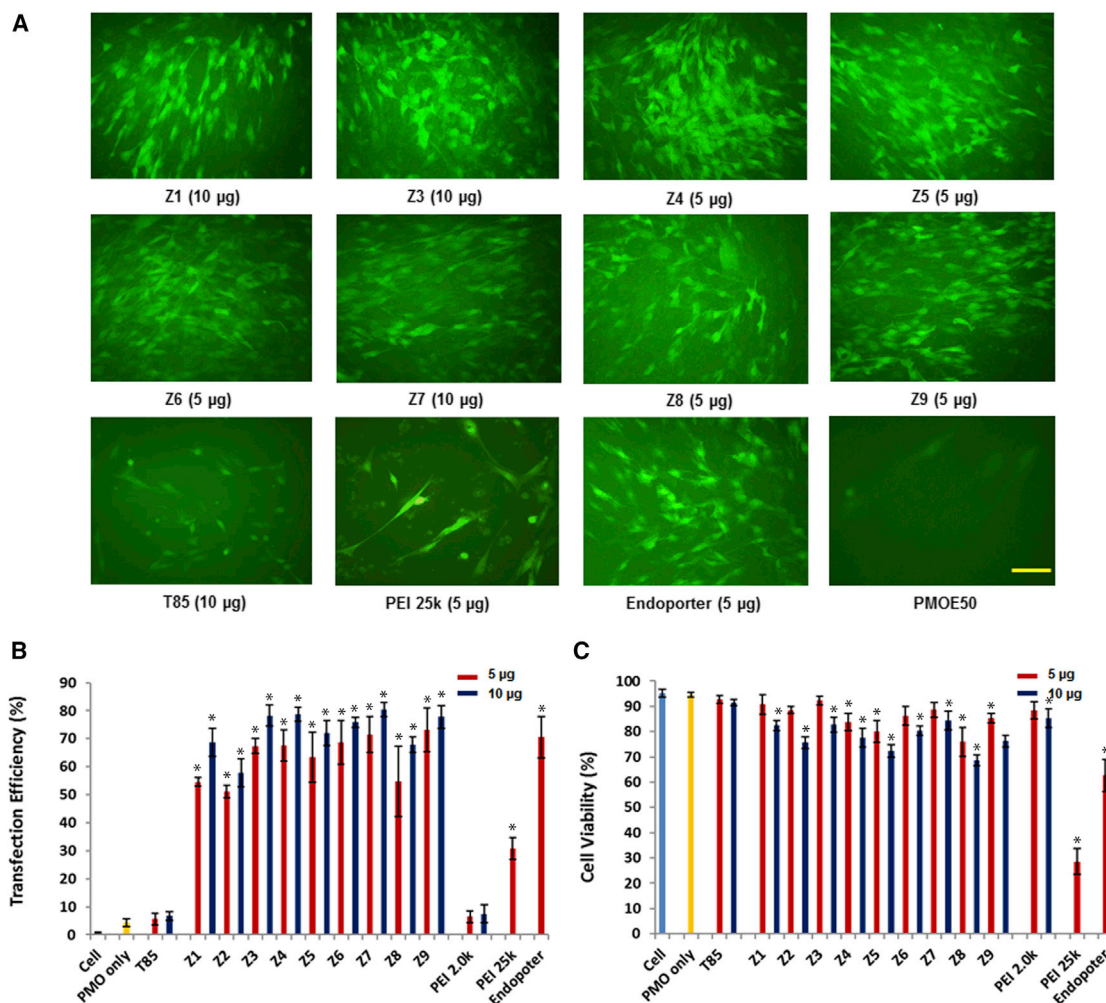
Figure 1. Delivery Efficiency and Toxicity of Z/PMOE50 Complexes in a C2C12E50 Cell Line Determined by Fluorescence Microscopy and Flow Cytometry Analysis

(A) Representative fluorescence images. The images were taken 4 days after treatment (original magnification, ×200; scale bar, 500 μm). (B) Statistical TE (n = 3, Mann-Whitney U test, *p ≤ 0.05 compared with PMO alone). (C) Cell viability (n = 3, Mann-Whitney U test, *p ≤ 0.05 compared with untreated cell). In this test, 5 μg PMOE50 was formulated with Zs, T85, or LPEI (5 and 10 μg), and PEI 25k (5 μg), Endo-porter (5 μg) formulated as comparison in 0.5 mL 10% FBS-DMEM medium, respectively.

Cell Uptake Study

To better understand how interaction of Z polymer with PMO enhances delivery efficiency, we directly visualized the uptake of Z7/3′-carboxyfluorescein-labeled PMO (FL-PMO) complex at a weight ratio of 5/2. The presence of Z7 and conformation of the polyplex apparently affects the pathway of the PMO uptake as demonstrated by confocal microscopy assay (Figure 3). PMO alone distributed almost entirely within the cytoplasm of the cells, consistent with a passive diffusion model of PMO uptake.[21] Blue-green signals (merged green and blue) were considerably stronger in the cells treated with Z7 formulated PMO, with concentrated signals appearing within the cytoplasm and accumulated perinuclear areas partly due to improved cell uptake of PMO complexed with Z7. This result reveals that PMO delivery promoted by the Z polymer is predomi-

nantly through enhanced endocytosis, which is in line well with the mechanism of polycation-mediated oligonucleotide delivery.[40–42]

Local Delivery of Z-Mediated PMO In Vivo

In view of the results that all Z polymers showed improved delivery performance for PMO exon-skipping, accompanied by much lower cytotoxicity compared with PEI 25k in vitro, we further evaluated them in vivo via intramuscular (i.m.) injection of PMOE23 formulated with Z polymers (including simple formulation and chemical conjugation) to tibialis anterior (TA) muscles of *mdx* mice (aged 4–5 weeks). The nonsense mutation in dystrophin exon 23 prevents production of a functional dystrophin protein, whereas targeted removal of the mutated exon by PMOE23 can restore the reading frame and
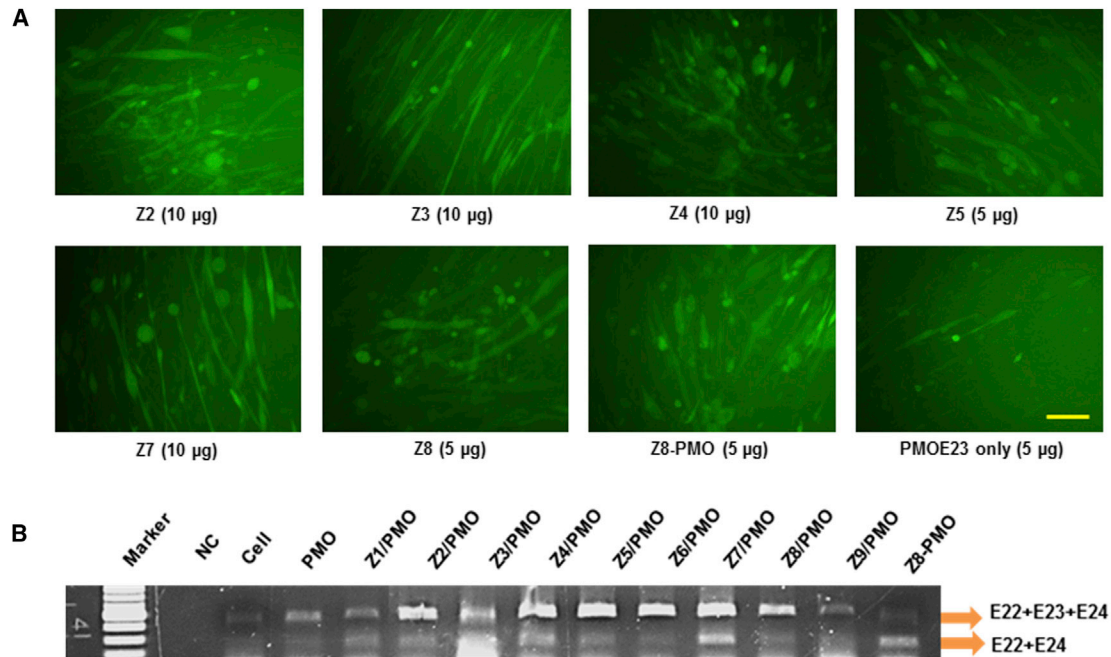
Figure 2. GFP Expression Induced by PMOE23 (5 μg) Formulated with Zs in C2C12E23 Cells (Zs [5 and 10 μg] and PMOE23 [5 μg], Z8-PMO [5 μg] in 0.5 mL of 10% FBS-DMEM after 6-day Treatment)

(A) Fluorescence detection of GFP expression (original magnification, ×200; scale bar, 500 μm). (B) RT-PCR of exon 23 skipping at the dose of 10 μg for polymer formulated with PMO (5 μg) and Z8-PMO (5 μg). The upper bands (424 bp, indicated by E22+E23+E24) correspond to the full length, and lower bands (213 bp, indicated by E22+E24) correspond to the exon 23 skipped mRNA.

expression of a functional dystrophin protein. Each TA muscle received 2 μg Z8-PMO, 2 μg PMOE23 formulated with 5 μg Z polymer, or PEI in 40 μL saline. The treated muscles were harvested 2 weeks after injection. Immunohistochemistry showed that PEI 2.0k, PEI 25k-formulated PMO, and PMO alone induced around 14%, 19%, and 11% dystrophin-positive fibers in one cross-section of the TA muscle, respectively. Dystrophin-positive fibers increased dramatically in the muscles treated with Z polymers formulated PMOE23. Dystrophin-positive fibers were 42%, 43%, 58%, 47%, 60%, 47%, and 71% with the use of Z2-, Z3-, Z5-, Z6-, Z7-, and Z9-formulated PMO and Z8-PMO conjugate, respectively. Most significantly, the Z5/Z7-formulated PMO and Z8-PMO conjugate reached increases of up approximately 6- to 7-fold compared with PMO alone (Figure 4). The levels of exon-skipping confirmed with RT-PCR were 26.9%, 23.1%, 44.8%, 17.8%, 34.9%, 35.6%, 39.7%, 20.1%, 28.7%, 37.6%, and 10.2% for Z1-, Z2-, Z3-, Z4-, Z5-, Z6-, Z7-, Z8-, and Z9-formulated PMO, Z8-PMO, and PMO only, respectively, and dystrophin expression further established with western blot displayed Z8-PMO, Z9 + PMO, and Z8 + PMO better than others. Percentage of dystrophin-positive fibers was clearly higher with the Z8-PMO conjugate (71%) when compared to Z8 + PMO (37%), which indicates that the conjugate Z8-PMO macromolecule holds more PMO loading efficiently, providing an advantage over the conventional nanoparticles produced by simple complexation. The lower delivery efficiency of Z8 compared to other Z polymers suggests that the more hydrophilic nature of the polymer does not conduct PMO de-

livery as a suitable carrier in vivo effectively. H&E staining revealed no signs of elevated inflammation or fiber degeneration and regeneration as compared to saline-treated controls, reaffirming their low tissue toxicity as demonstrated previously for pDNA and 2'-OMePS delivery.[33,34]

Systemic Delivery of Z-Mediated PMO In Vivo

DMD is a systemic disease affecting body-wide muscles including cardiac muscle; therefore, systemic administration is essential for treatment. Based on the preliminary results in vitro and in vivo locally, we selected the effective and safe polymer Z7 as simple formulation with PMO (Z7 + PMO) and Z8-PMO as chemical formulation to evaluate the systemic consequence by intravenous (i.v.) injection (1 mg Z7/1 mg PMO complex, 0.5/1 mg Z8-PMO conjugate, and 1 mg PMO as control). The PMO alone induced dystrophin expression in less than 3% of muscle fibers in all skeletal muscles, and there was no detectable dystrophin in cardiac muscle when examined 2 weeks after injection. Z7/PMO complex produced dystrophin-positive fibers up to 10% in almost all skeletal muscles examined (Figure 5). More importantly, the Z8-PMO conjugate achieved dystrophin-positive fibers 2- to 4-fold higher than the Z7/PMO simple formulation in skeletal muscles reaching 28%, 25%, 26%, and 41% in TA, gastrocnemius, intercostal, and diaphragm, respectively. This is partly due to the advantage of single-molecule Z8-PMO with better distribution and stability in the circulatory system. The size and uniformity of Z8-PMO conjugate could also be advantageous to
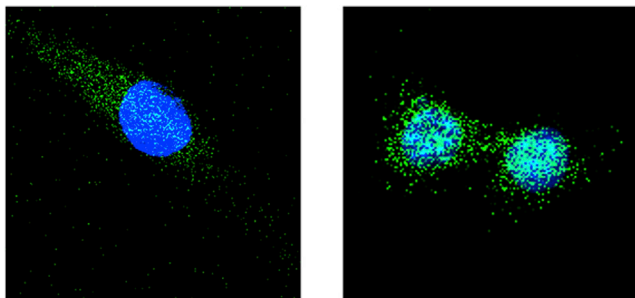
Figure 3. Confocal Photomicrographs of C2C12 Cells Incubated with Z7 (5 μg) Formulated FL-PMO (2 μg) in 0.5 mL Medium and Nuclear Counterstaining with Hoechst 33258

The images (left, FL-PMO only; right, Z7/FL-PMO complex) were obtained under a magnification of ×63. Location of FL-PMO can be observed in both images by distribution of (green) signal, while nuclear counterstain (blue) clearly demonstrates the different pattern and PMO levels in passive uptake associated with naked PMO and the promoted uptake when PMO is complexed with the Z7 polymer.

penetrating through the muscle vasculature but avoiding quick renal filtration. Dose dependency was also observed when compared 1 mg Z8-PMO with 0.5 mg Z8-PMO as determined by RT-PCR and western blot. Transcripts with exon 23 skipped and the levels of dystrophin protein were improved in both TA and diaphragm muscles in Z8-PMO-conjugate-treated mice. Most notably, immunohistochemistry demonstrated membrane-localized dystrophin-positive fibers in some areas of the heart. This is important and promising, since cardiomyopathy due to lack of dystrophin expression is currently the leading cause of death among DMD patients, and restoration of dystrophin even at low levels could delay disease progression in DMD.[2,43,44]

During the treatment with the Z/PMO simple formulation or Z-PMO conjugate, no sign of abnormal behavior and change in body weight were observed in systemic delivery under the tested dosage. Histological examination revealed no pathological changes in skeletal muscles, liver, kidney, and lung of the treated mice compared to the untreated *mdx* mice by H&E staining. This was consistent with the serum test results (Figure 6): urea nitrogen, total bilirubin, calcium, alkaline phosphatase, and γ-glutamyltransferase were in normal range, whereas significant reduction in the levels of creatine kinase and alanine transamines were found with the 1 mg Z8-PMO-treated mice against untreated *mdx* mice.

Our results consequently suggest that modification of PMO with Z polymers both in simple formulation and chemical conjugation has the potential to increase exon-skipping of PMO for all skeletal and cardiac muscle and further confirming the advantage of chemically covalent conjugate, though additional optimization is required. These results, together with the lack of detectable toxicity in muscles, liver, and kidney after systemic treatment further solidify the potential of amphiphilic polymers as PMO delivery-enhancing carriers for the treatment of muscular dystrophies with long-term administration.

Affinity Study between Polymer and PMO

The affinity between polymer and oligonucleotides is important for the formation of appropriate particle size, density, and surface charge and, consequently, the stability of the complex, their uptake and release at proper time and location, and finally, delivery efficiency.[36,45–48] To better clarify the delivery action of polymer-mediated PMO in vitro and in vivo, we examined the polymer Z8, Z8/PMO polyplex, and Z8-PMO conjugate under transmission electron microscopy (TEM) and UV-Vis study. As illustrated in Figure 7A, the polymer Z8 alone formed smaller particles with different sizes via self-assembly because of its amphiphilic properties, while the PMO alone formed below 50-nm particles that are most likely a result of hydrophobic interactions among PMO molecules. On the other hand, the polyplex of Z8/PMO at a weight ratio of 10/5 (based on the in vitro results) condensed spherical particles with an average diameter of around 40–70 nm, likely due to the hydrophobic interaction and hydrogen bonds between the PMO and polymer,[31–35] whereas the Z8-PMO conjugate produced particles with even sizes between 10 and 20 nm, much smaller than simple formulation. The interactions were further examined by UV-Vis spectrum (Figure 7B): the Z8 alone gave absorbance around 230 nm and PMO at 262 nm, Z8-PMO conjugate displayed similar absorbance as PMO alone, and the Z8/PMO formulation showed broad hypochromic effect and hypsochromic shift as compared to Z8-PMO or PMO alone. Z8's absorbance was shielded in either Z8-PMO conjugate or Z8/PMO simple formulation. These results indicated the strong interaction between Z polymer and PMO even though they are not chemically conjugated. Furthermore, the stronger hyperchromic effect of Z-PMO conjugate relative to Z/PMO simple formulation is probably due to the high PMO loading efficiency and nanoparticle homogeneity of chemical conjugation, leading to superior performances than conventional formulation both in bio-distribution and stability.

Conclusions

The study of T85-modified LPEI amphiphilic polymers for antisense PMO delivery in vitro and in *mdx* mice demonstrated that the polymer's performance as delivery carrier is related to the molecular size, composition, and hydropholic-lipopholic balance (HLB), as well as the delivery strategy. In general, the polymers with moderate size and higher PEI content or large molecular size are preferred as PMO delivery carriers. The best formulation results in PMO delivery efficiency 20- and 6-fold of that with PMO alone in vitro and in vivo, respectively. The variability of individual Z polymers for delivery of negatively charged pDNA/2′-OMePS and uncharged PMO highlighted the complexity of the interaction between the polymer and the therapeutic agents, the difference in the delivery mechanism. The unique hydrophobic interaction between the Z polymer and PMO creates a more stable complex in primarily hydrophilic environments and further enhances complex-plasma membrane interactions both in vitro and in vivo. For the simple formulation, all the Zs have lower toxicity as compared with Endo-porter and PEI 25k. Improved exon-skipping efficiency was observed in vitro with all Z polymers, and some of them exhibit efficiency comparable to or higher than Endo-porter. The degree of efficiency was found in the order of Z3,
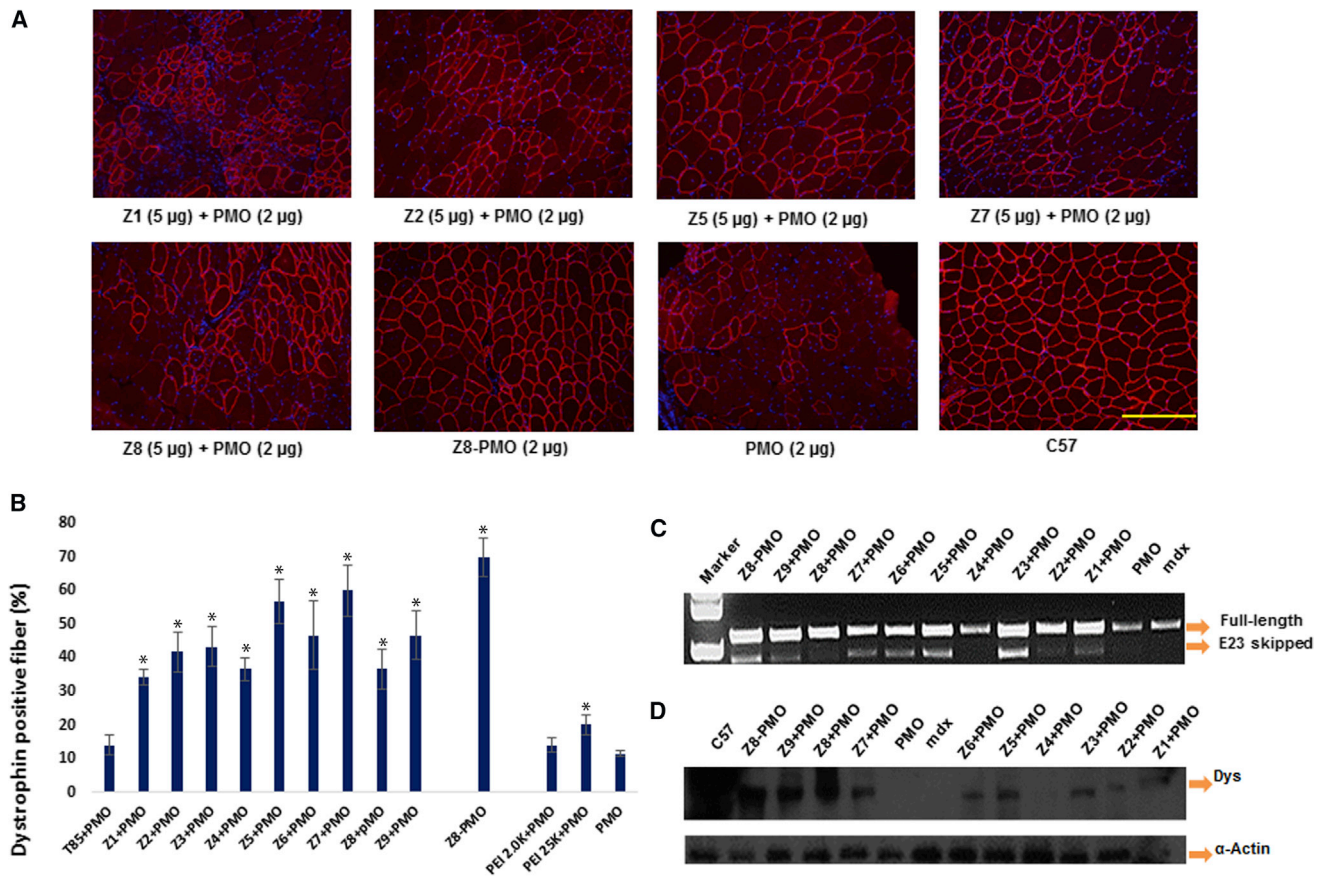
Figure 4. Restoration of Dystrophin in Tibialis Anterior Muscles of *mdx* Mice Aged 4–5 Weeks 2 Weeks after Intramuscular Injection

Muscles treated with PMOE23 only were used as controls; all other samples were from muscles treated with 5 μg polymer formulated with 2 μg PMOE23 or 2 μg Z8-PMO in 40 μL saline. (A) Dystrophin was detected by immunohistochemistry with rabbit polyclonal antibody P7 against dystrophin. Blue nuclear staining with 4,6-diamidino-2-phenylindole (original magnification, ×200; scale bar, 200 μm). (B) The percentage of dystrophin-positive fibers. The number of dystrophin-positive fibers was counted in a single cross-section (n = 5, two-tailed Student's t test, *p ≤ 0.05 compared with PMO). (C) Detection of exon 23 skipping by RT-PCR. Total RNA of 100 ng from each sample was used for amplification of dystrophin mRNA from exon 20 to exon 26. The upper bands (1,093 bp) correspond to the normal mRNA, and the lower bands (880 bp) correspond to the mRNA with exon E23 skipped. (D) Western blots demonstrate the expression of dystrophin protein from treated *mdx* mice in comparison with C57BL/6 and untreated *mdx* mice (10 μg of total protein was loaded for PMO/modified PMO and control *mdx* samples; 10 μg for the wild-type (WT) C57 control also). Dys, dystrophin detected with monoclonal antibody Dys 1. α-Actin used as the loading control.

Z4, Z7 ≥ Z9, Z6 > Z1, and Z5 > others at the dose of 20 μg/mL. The in vivo study in *mdx* mice demonstrated significantly enhanced exon-skipping of PMO with the Z polymers in the order of Z7 > Z5 > Z2, Z3, Z6, and Z9 > others. Most important, the Z8-PMO conjugate validated superior performances to simple formulation both in vitro and in vivo, highlighting the advantage of single molecular nanocarriers with better bio-distribution and stability.

MATERIALS AND METHODS

DMEM, penicillin-streptomycin, fetal bovine serum (FBS), L-glutamine, and HEPES (4-(2-hydroxyethyl)-1-piperazineethane-sulfonic acid) buffer solution (1 M) were purchased from Gibco, Invitrogen (USA). All other chemicals were reagent grade. PMO PMOE50 (5′-AACTTCCTCTTTAACAGAAAAGCA TAC-3′), PMOE23 (+07–18) (5′-GGCCAAACCTCGGCTTACCT

GAAAT-3′), and Endo-porter were purchased from Gene Tools (Philomath, OR, USA). The Z polymers were prepared previously by us,[33,34] and Z-PMO conjugation was prepared as procedure reported by Ming X et al., with a little modification (see Supplemental Information).[37]

In Vitro Transfection

C2C12E50 or C2C12E23 cells were cultured in DMEM and maintained at 37°C and 10% CO_2 in a humidified incubator. 5×10^4 cells per well were seeded in a 24-well plate in 500 μL medium containing 10% FBS and allowed to reach 70%–80% confluence prior to transfection. Cell culture medium was replaced prior to addition of polymer/PMO (fixed at 5 μg) formulated with varying ratio. PEI 25k and Endo-porter were used as delivery controls. Transfection efficiencies were recorded with the Olympus IX71 fluorescent microscope
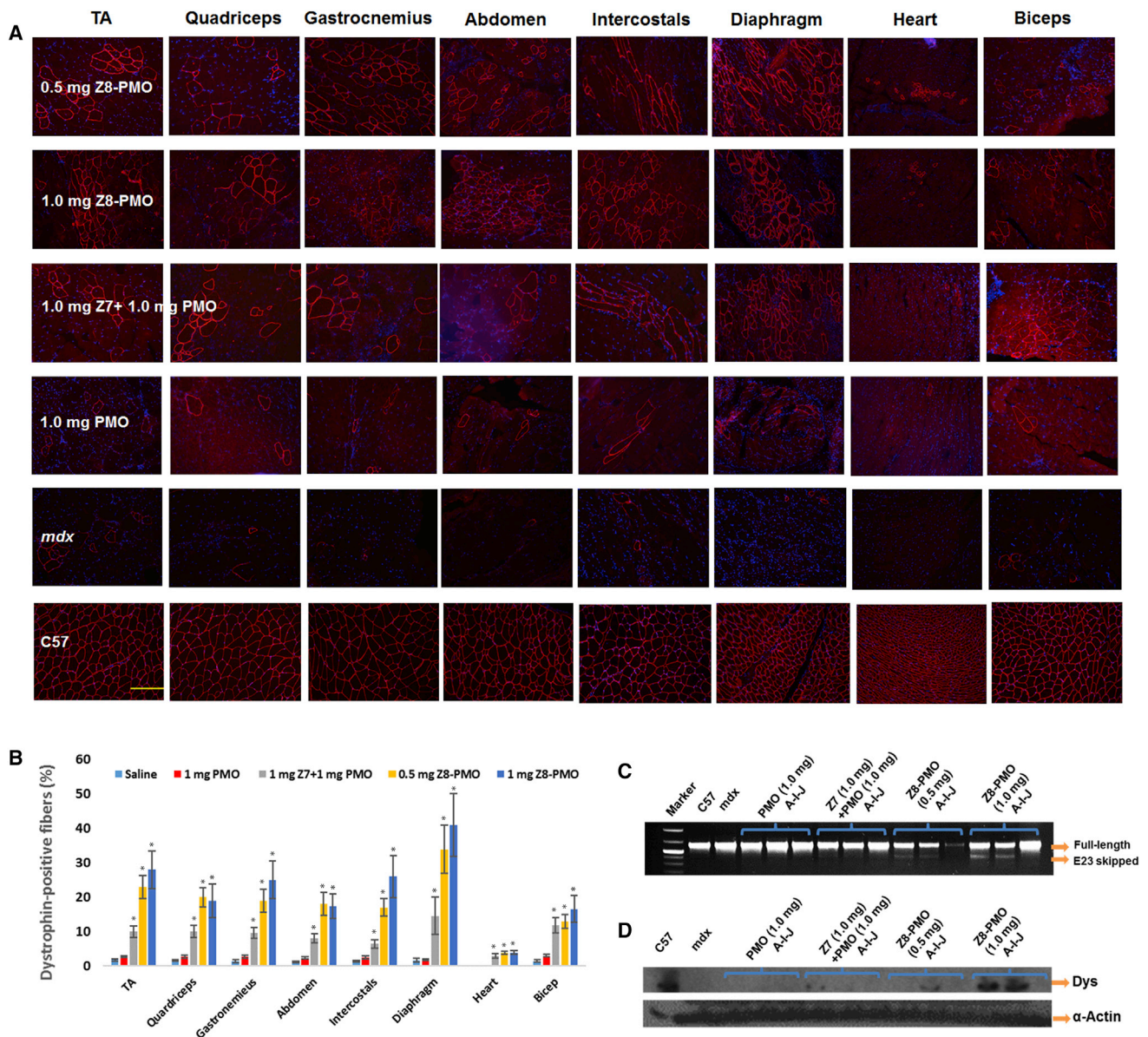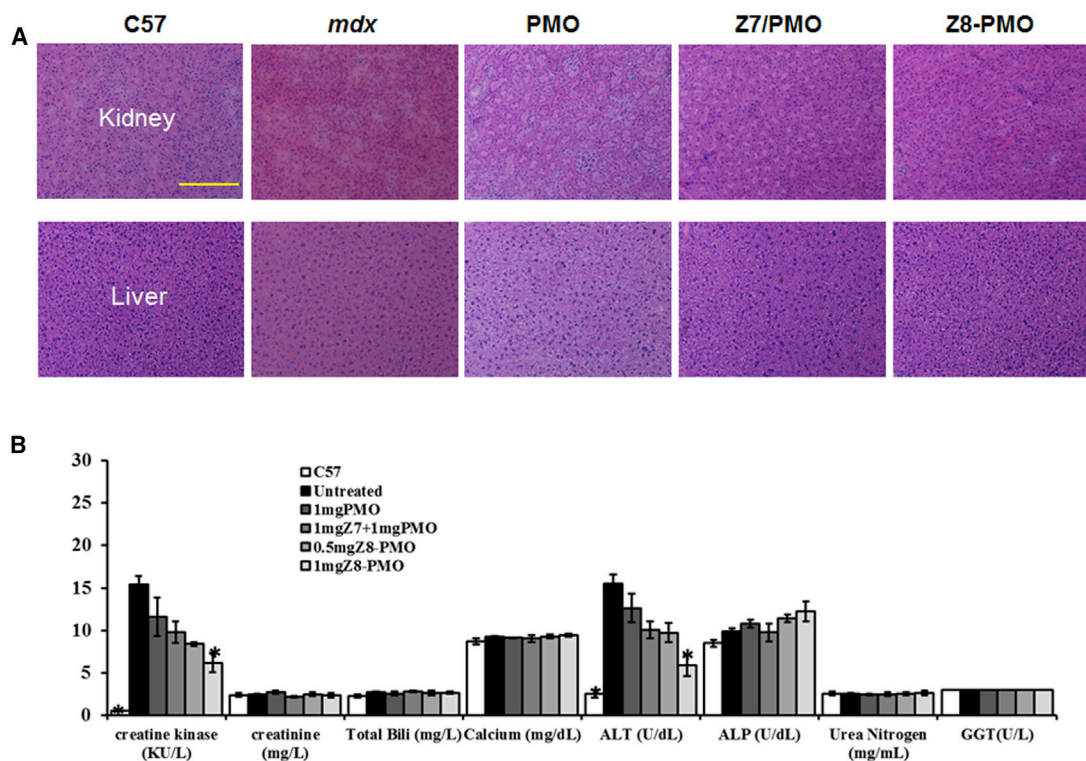
Figure 5. Restoration of Dystrophin Expression after 2-Week Systemic Delivery of Z Polymer-Formulated PMO or Z-PMO Conjugate in *mdx* Mice Aged 4–5 Weeks

PMO (1 mg) only was used as controls. All other samples were from muscles treated with polymer-conjugated or simple formulated PMO (0.5 or 1 mg) in 100 µL saline. (A) Dystrophin was detected by immunohistochemistry with rabbit polyclonal antibody P7 against dystrophin. Blue nuclear staining with 4,6-diamidino-2-phenylindole (original magnification, ×200; scale bar, 200 µm). (B) The percentage of dystrophin-positive fibers in muscles treated with conjugated or simple formulated PMO. The numbers of dystrophin-positive fibers were counted in a single cross-section (n = 5, two-tailed Student's t test, *p ≤ 0.05 compared with 1 mg PMO). (C) Detection of exon 23 skipping by RT-PCR. Total RNA of 100 ng from each sample was used for amplification of dystrophin mRNA from exon 20 to exon 26. The upper bands correspond to the normal mRNA, and the lower bands correspond to the truncated mRNA with exon E23 skipped. (D) Western blots demonstrate the expression of dystrophin protein from treated *mdx* mice in comparison with C57BL/6 and untreated *mdx* mice (50 µg of total protein was loaded for PMO/modified PMO and control *mdx* samples; 12.5 µg for the WT C57 control. A, TA; I, diaphragm; J, heart; Dys, dystrophin detected with monoclonal antibody Dys 1. α-Actin was used as the loading control.

(Olympus America, Melville, NY, USA). TE was examined quantitatively using flow cytometry (BD, Franklin Lakes, NJ, USA), and the exon-skipping was also further examined by RT-PCR in the C2C12E23 cell line.[31–35,39] One hundred nanograms of template RNA was used for each 25 µL RT-PCR reaction. The primer sequences for the RT-PCR were EGFP5′, 5′-CAGAATTCTGC CAATTGCTGAG-3′ and EGFP3′, 5′-TTCTTCAGCTTGTGT CATCC-3′. The cycle conditions for reverse transcription were

Figure 6. Examination of Pathology and Serum after 2-Week Systemic Delivery of Z Polymer-Formulated PMO or Z-PMO Conjugate in *mdx* Mice Aged 4–5 Weeks

PMO (1 mg) only was used as controls. All other samples were from muscles treated with polymer-conjugated or simple formulated PMO (0.5 or 1 mg) in 100 μL saline. (A) H&E staining of liver and kidney tissue from the normal C57BL/6 mice, untreated mdx mice, PMO-, Z/PMO-, and Z-PMO-treated *mdx* mice (1 mg PMO, 1 mg Z7/1 mg PMO, 1 mg Z8-PMO; original magnification, ×200; scale bar, 200 μm). (B) The levels of serum enzymes, creatine kinase (KU/L), creatinine (mg/L), urea nitrogen (mg/mL), total bilirubin (mg/L), calcium (mg/dL), alanine transaminase (ALT) (U/dL), alkaline phosphatase (ALP) (U/dL), and ɤ-glutamyltransferase (GGT) (U/L). n = 5; *p ≤ 0.05 compared with untreated *mdx* mice. Two-tailed Student's t test.

43°C for 15 min, 94°C for 2 min. The reaction was then cycled 30 times at 94°C for 30 s, 65°C for 30 s, and 68°C for 1 min. The intensity of the bands was measured with ImageJ software version 1.42 (National Institutes of Health, Bethesda, MD), and the percentage of exon-skipping was calculated with the intensity of the two bands representing both exon 23 unskipped and skipped as 100%. Unskipped band including exon 23 is 424 bp; skipped band without exon 23 is 213 bp.

Cellular Uptake

C2C12 cells were seeded onto 8-well glass Lab-Tek II chamber slides (Scientific, Ocala, FL, USA) at 5×10^3 cells/well, cultured to 70% confluence before the addition of polymer/fluorophore-labeled PMO formulation at predetermined ratios. Cultures were incubated another 24 hr after addition of the samples, and cells were washed with warm PBS to remove any residual polymer/PMO polyplex from cells and equilibrated by incubation with fresh medium. Cells were counterstained with Hoechst 33528 (Life Technologies, Carlsbad, CA, USA) to label cellular nuclei, then examined under Zeiss LSM-710 inverted confocal microscope (Carl Zeiss Microscopy,

Thornwood, NY, USA), and the resulting images were analyzed for uptake and localization by single-channel images. Co-localization of polymer/PMO to the lysosome was visualized by merged channel images to assess the signal intensities of the labeled PMO and lysosomes relative to the counterstained nuclei.

In Vivo AO Delivery

This study was carried out in strict accordance with the recommendations in the National Institutes of Health Guide for the Care and Use of Laboratory Animals. The protocols were approved by the Institutional Animal Care and Use Committee (IACUC), Carolinas Medical Center (breeding protocol 10-13-07A; experimental protocol 10-13-08A). The mice were housed in temperature controlled between 70°F and 74°F, and a 12/12 of light/dark cycle. Food and water were available ad libitum during the whole study. Environmental enrichment was a cardboard tube, wood block (Bio-serv), Crink-l'Nest (Anderson), a nestlet, and once a week rodent foraging crumbles (Bio-serv). The mice were free of standard pathogens. We allocated pups from same mouse parents into different groups. All injections were performed under isoflurane anesthesia, and all efforts were made to minimize suffering.[9,15,16]
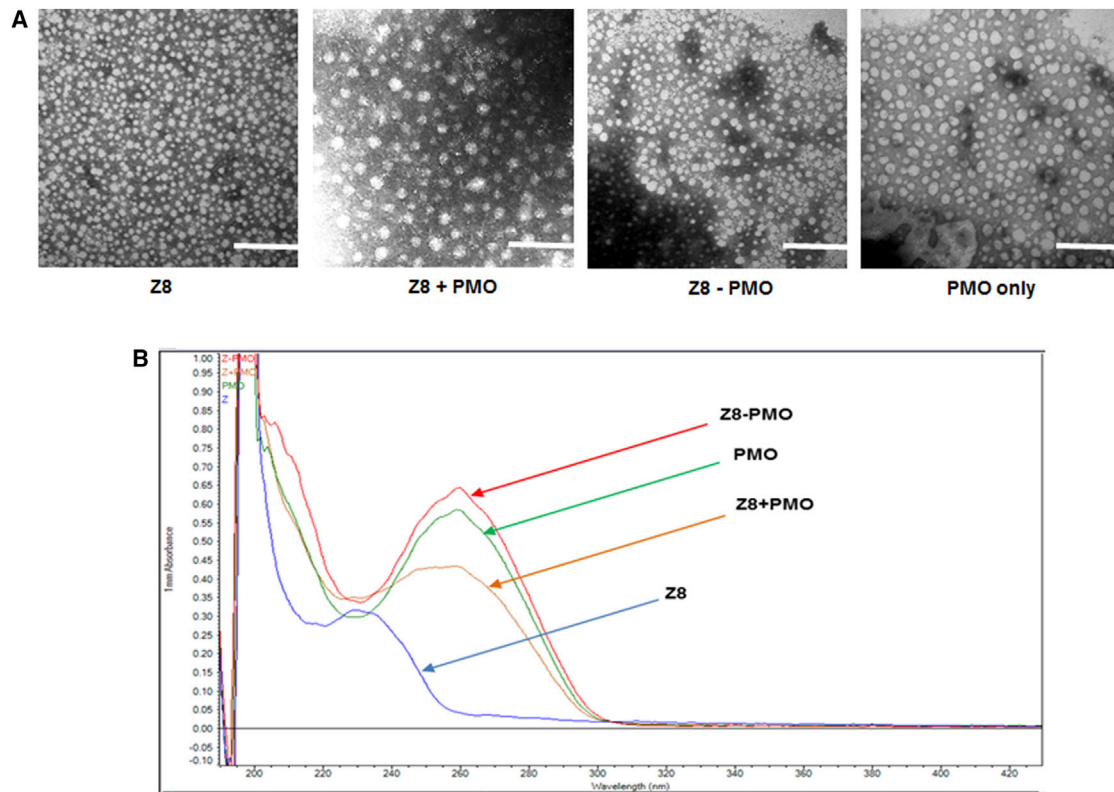
Figure 7. Affinity Study between Polymer and PMO

(A) Negatively stained transmission electron micrographs (scale bar, 200 nm) of Z8 (2 μg), PMO (1 μg), Z8 (2 μg) complexed with PMO (1 μg), and Z8-PMO conjugate (1 μg). (B) UV-Vis spectra (Z8, 1 mg/mL; PMO/Z8-PMO, 0.5 mg/mL in deionized (DI) water, 1.5 μL sample measured at room temperature).

Animals and Injections

Dystrophic *mdx* mice (C57BL/10 as genetic background) aged 4–5 weeks were used for in vivo testing (5 mice [2 female + 3 male] each in the test and control groups) unless otherwise stated. Mice were killed by CO_2 inhalation at desired time points, and muscles and other tissues were snap frozen in liquid-nitrogen-cooled isopentane and stored at −80°C. The PMOE23 targeting the boundary sequences of exon and intron 23 of mouse dystrophin gene (Gene Tools, Philomath, OR) was used. For i.m. injections, 2 μg Z-PMOE23 conjugate or 2 μg PMOE23 formulated with polymer (5 μg) in 40 μL saline was applied for each tibialis anterior (TA) muscle. For i.v. injection, 0.5 or 1 mg Z-PMOE23 conjugate or 1 mg PMOE23 formulated with 1 mg polymer in 100 μL saline was used. The muscles were examined 2 weeks later, and all of tissues were processed with the operator blinded to the treatment groups.

Immunohistochemistry and Histology

Serial sections of 6 μm were cut from the treated mouse muscles. The sections were stained with a rabbit polyclonal antibody P7 for the detection of dystrophin protein as described previously.[15,16,31–35] Polyclonal antibodies were detected by goat anti-rabbit immunoglobulin G (IgG) Alexa 594 (Invitrogen, Carlsbad, CA). As for dystrophin-positive fiber counting, the number of dystrophin-positive fibers in one section was addressed using the Olympus BX51 fluorescent microscope (Olympus America, Melville, NY, USA). Sections were also stained with H&E for histological assessment.

Western Blot and RT-PCR for In Vivo Samples

Protein extraction and western blot were done as described previously.[15,16] The collected sections were ground into powder, and lysed with 200 μL protein extraction buffer (1% Triton X-100, 50 mM Tris [pH 8.0], 150 mM NaCl, 0.1% SDS), boiled at 100°C in water for 1 min, then centrifuged at $18,000 \times g$ at 4°C for 15 min. The supernatants were quantified for the protein concentration with a protein assay kit (Bio-Rad Laboratories, Hercules, CA). Proteins were loaded onto a 4% to 15% Tris-HCL gradient gel. Samples were electrophoresed 4 hr at 120 V at room temperature (RT). Then the gel blotted onto nitrocellulose membrane for 4 hr at 150 V at 4°C. The membrane was probed with NCL-DYS1 monoclonal antibody against dystrophin rod domain (1:200 dilutions, Vector Laboratories, Burlingame, CA). The bound primary antibody was detected by horseradish peroxidase (HRP)-conjugated goat anti-mouse IgG (1:3,000 dilutions, Santa Cruz Biotechnology, Santa Cruz, CA) and the ECL Western Blotting Analysis System (Perkin-Elmer, Waltham, MA). The intensity of the bands obtained from the treated *mdx* mouse muscles was measured and compared with that from normal

muscles of C57BL/6 mice (ImageJ software version 1.42; National Institutes of Health, Bethesda, MD). α-actin was detected by rabbit anti-actin antibody (Sigma, St. Louis, MO) as a sample loading control.

Total RNA was extracted from the muscle after dissection, and 100 ng of RNA template was used for a 50 μL RT-PCR with the Stratascript One-Tube RT-PCR System (Stratagene, Santa Clara, CA). Ex20Fo 5′-AGAATTCTGCCAATTGCTGAG-3′ and Ex26Ro 5′-TCTTCAG CTTGTGTCATCC-3′ for amplification of mRNA from exons 20 to 26. Unskipped band including exon 23 is 1093 bp; skipped band without exon 23 is 880 bp.

Measurement of Serum Creatine Kinase and Other Components
Mouse blood was taken immediately after cervical dislocation and centrifuged at 1,500 rpm for 10 min. Serum was separated and stored at −80°C. The level of serum components was determined by IDEXX Laboratories (North Grafton, MA, USA).

TEM
The polymer/PMO polyplex solution containing 1 μg of PMO was prepared at weight ratio of 2/1 (polymer/PMO) in 0.1 mL medium, as were the corresponding polymer and PMO only as comparison, analyzed using TEM (Phllips CM-10, Philips Electronics North America, Andover, MA, USA). The samples were prepared with negative staining by 1% phosphotungstic acid.[31–35]

UV-Vis Study
NanoDrop 2000 spectrophotometer (Thermo Scientific, Waltham, MA USA) was used to determine the absorbance of polymer and PMO in both simple formulation or chemical conjugation. One and one-half microliters of each sample was measured at the desired concentration under RT.

Statistical Analysis
The statistical analysis of experimental data was evaluated using a Mann-Whitney U test and two-tailed Student's t test, and results were reported as mean values ± SEM; statistical significance was accepted when *p ≤ 0.05.

SUPPLEMENTAL INFORMATION
Supplemental Information includes one scheme and one figure and can be found with this article online at https://doi.org/10.1016/j.omtn.2017.09.006.

AUTHOR CONTRIBUTIONS
M.W. and Q.L. conceived and designed the experiments; M.W. wrote the paper and performed the whole experiment except for the in vivo study; B.W. supervised and performed the in vivo experiments with S.N.S. and L.E.B.; J.D.T. and P.L. contributed to cell culture; Q.L., B.W., and J.D.T. reviewed the manuscript.

CONFLICTS OF INTEREST
The authors declare no conflicts of interest in relation to this paper.

REFERENCES
1. Hoffman, E.P., Brown, R.H., Jr., and Kunkel, L.M. (1987). Dystrophin: the protein product of the Duchenne muscular dystrophy locus. Cell 51, 919–928.
2. Wagner, K.R., Lechtzin, N., and Judge, D.P. (2007). Current treatment of adult Duchenne muscular dystrophy. Biochim. Biophys. Acta 1772, 229–237.
3. Emery, A.E.H. (1993). Duchenne Muscular Dystrophy (Oxford Medical Publications).
4. Mendell, J.R., Shilling, C., Leslie, N.D., Flanigan, K.M., al-Dahhak, R., Gastier-Foster, J., Kneile, K., Dunn, D.M., Duval, B., Aoyagi, A., et al. (2012). Evidence-based path to newborn screening for Duchenne muscular dystrophy. Ann. Neurol. 71, 304–313.
5. Long, C., Amoasii, L., Mireault, A.A., McAnally, J.R., Li, H., Sanchez-Ortiz, E., Bhattacharyya, S., Shelton, J.M., Bassel-Duby, R., and Olson, E.N. (2016). Postnatal genome editing partially restores dystrophin expression in a mouse model of muscular dystrophy. Science 351, 400–403.
6. Lu, Q.L., Cirak, S., and Partridge, T. (2014). What can we learn from clinical trials of exon skipping for DMD? Mol. Ther. Nucleic Acids 3, e152.
7. Kole, R., and Krieg, A.M. (2015). Exon skipping therapy for Duchenne muscular dystrophy. Adv. Drug Deliv. Rev. 87, 104–107.
8. Koo, T., and Wood, M.J. (2013). Clinical trials using antisense oligonucleotides in duchenne muscular dystrophy. Hum. Gene Ther. 24, 479–488.
9. Wu, B., Moulton, H.M., Iversen, P.L., Jiang, J., Li, J., Li, J., Spurney, C.F., Sali, A., Guerron, A.D., Nagaraju, K., et al. (2008). Effective rescue of dystrophin improves cardiac function in dystrophin-deficient mice by a modified morpholino oligomer. Proc. Natl. Acad. Sci. USA 105, 14814–14819.
10. van Deutekom, J.C., Janson, A.A., Ginjaar, I.B., Frankhuizen, W.S., Aartsma-Rus, A., Bremmer-Bout, M., den Dunnen, J.T., Koop, K., van der Kooi, A.J., Goemans, N.M., et al. (2007). Local dystrophin restoration with antisense oligonucleotide PRO051. N. Engl. J. Med. 357, 2677–2686.
11. Kinali, M., Arechavala-Gomeza, V., Feng, L., Cirak, S., Hunt, D., Adkin, C., Guglieri, M., Ashton, E., Abbs, S., Nihoyannopoulos, P., et al. (2009). Local restoration of dystrophin expression with the morpholino oligomer AVI-4658 in Duchenne muscular dystrophy: a single-blind, placebo-controlled, dose-escalation, proof-of-concept study. Lancet Neurol. 8, 918–928.
12. Goemans, N.M., Tulinius, M., van den Akker, J.T., Burm, B.E., Ekhart, P.F., Heuvelmans, N., Holling, T., Janson, A.A., Platenburg, G.J., Sipkens, J.A., et al. (2011). Systemic administration of PRO051 in Duchenne's muscular dystrophy. N. Engl. J. Med. 364, 1513–1522.
13. Cirak, S., Arechavala-Gomeza, V., Guglieri, M., Feng, L., Torelli, S., Anthony, K., Abbs, S., Garralda, M.E., Bourke, J., Wells, D.J., et al. (2011). Exon skipping and dystrophin restoration in patients with Duchenne muscular dystrophy after systemic phosphorodiamidate morpholino oligomer treatment: an open-label, phase 2, dose-escalation study. Lancet 378, 595–605.
14. Yin, H., Moulton, H.M., Seow, Y., Boyd, C., Boutilier, J., Iversen, P., and Wood, M.J. (2008). Cell-penetrating peptide-conjugated antisense oligonucleotides restore systemic muscle and cardiac dystrophin expression and function. Hum. Mol. Genet. 17, 3909–3918.
15. Wu, B., Lu, P., Benrashid, E., Malik, S., Ashar, J., Doran, T.J., and Lu, Q.L. (2010). Dose-dependent restoration of dystrophin expression in cardiac muscle of dystrophic mice by systemically delivered morpholino. Gene Ther. 17, 132–140.

16. Wu, B., Lu, P., Cloer, C., Shaban, M., Grewal, S., Milazi, S., Shah, S.N., Moulton, H.M., and Lu, Q.L. (2012). Long-term rescue of dystrophin expression and improvement in muscle pathology and function in dystrophic *mdx* mice by peptide-conjugated morpholino. Am. J. Pathol. *181*, 392–400.

17. Sirsi, S.R., Schray, R.C., Guan, X., Lykens, N.M., Williams, J.H., Erney, M.L., and Lutz, G.J. (2008). Functionalized PEG-PEI copolymers complexed to exon-skipping oligonucleotides improve dystrophin expression in mdx mice. Hum. Gene Ther. *19*, 795–806.

18. Lee, M., Rentz, J., Bikram, M., Han, S., Bull, D.A., and Kim, S.W. (2003). Hypoxia-inducible VEGF gene delivery to ischemic myocardium using water-soluble lipopolymer. Gene Ther. *10*, 1535–1542.

19. Dowling, J.J. (2016). Eteplirsen therapy for Duchenne muscular dystrophy: skipping to the front of the line. Nat. Rev. Neurol. *12*, 675–676.

20. Aartsma-Rus, A., and Krieg, A.M. (2017). FDA approves eteplirsen for Duchenne muscular dystrophy: The next chapter in the eteplirsen saga. Nucleic Acid Ther. *27*, 1–3.

21. Summerton, J., and Weller, D. (1997). Morpholino antisense oligomers: design, preparation, and properties. Antisense Nucleic Acid Drug Dev. *7*, 187–195.

22. Kendall, G.C., Mokhonova, E.I., Moran, M., Sejbuk, N.E., Wang, D.W., Silva, O., Wang, R.T., Martinez, L., Lu, Q.L., Damoiseaux, R., et al. (2012). Dantrolene enhances antisense-mediated exon skipping in human and mouse models of Duchenne muscular dystrophy. Sci. Transl. Med. *4*, 164ra160.

23. Cao, L., Han, G., Lin, C., Gu, B., Gao, X., Moulton, H.M., Seow, Y., and Yin, H. (2016). Fructose promotes uptake and activity of oligonucleotides with different chemistries in a context-dependent manner in *mdx* mice. Mol. Ther. Nucleic Acids *5*, e329.

24. Han, G., Gu, B., Cao, L., Gao, X., Wang, Q., Seow, Y., Zhang, N., Wood, M.J., and Yin, H. (2016). Hexose enhances oligonucleotide delivery and exon skipping in dystrophin-deficient mdx mice. Nat. Commun. *7*, 10981.

25. Pack, D.W., Hoffman, A.S., Pun, S., and Stayton, P.S. (2005). Design and development of polymers for gene delivery. Nat. Rev. Drug Discov. *4*, 581–593.

26. Lu, Q.L., Bou-Gharios, G., and Partridge, T.A. (2003). Non-viral gene delivery in skeletal muscle: a protein factory. Gene Ther. *10*, 131–142.

27. Lemieux, P., Guérin, N., Paradis, G., Proulx, R., Chistyakova, L., Kabanov, A., and Alakhov, V. (2000). A combination of poloxamers increases gene expression of plasmid DNA in skeletal muscle. Gene Ther. *7*, 986–991.

28. Pitard, B., Pollard, H., Agbulut, O., Lambert, O., Vilquin, J.T., Cherel, Y., Abadie, J., Samuel, J.L., Rigaud, J.L., Menoret, S., et al. (2002). A nonionic amphiphile agent promotes gene delivery in vivo to skeletal and cardiac muscles. Hum. Gene Ther. *13*, 1767–1775.

29. Cho, K.C., Choi, S.H., and Park, T.G. (2006). Low molecular weight PEI conjugated pluronic copolymer: useful additive for enhancing gene transfection efficiency. Macromol. Res. *14*, 348–353.

30. Nguyen, H.K., Lemieux, P., Vinogradov, S.V., Gebhart, C.L., Guérin, N., Paradis, G., Bronich, T.K., Alakhov, V.Y., and Kabanov, A.V. (2000). Evaluation of polyether-polyethyleneimine graft copolymers as gene transfer agents. Gene Ther. *7*, 126–138.

31. Wang, M., Wu, B., Lu, P., Cloer, C., Tucker, J.D., and Lu, Q. (2013). Polyethylenimine-modified pluronics (PCMs) improve morpholino oligomer delivery in cell culture and dystrophic *mdx* mice. Mol. Ther. *21*, 210–216.

32. Wang, M., Wu, B., Tucker, J.D., Lu, P., Cloer, C., and Lu, Q.L. (2014). Evaluation of Tris[2-(acryloyloxy)ethyl]isocyanurate cross-linked polyethylenimine as antisense morpholino oligomer delivery vehicle in cell culture and dystrophic *mdx* mice. Hum. Gene Ther. *25*, 419–427.

33. Wang, M.X., Wu, B., Tucker, J.D., Lu, P., Shah, S.N., Wade, S., and Lu, Q.L. (2014). Synthesis and evaluation of Tween 85-LPEI copolymers for gene transfection in vitro and in vivo. J. Nanomed. Nanotechnol. *5*, 228.

34. Wang, M.X., Wu, B., Tucker, J.D., Lu, P., Bollinger, L.E., and Lu, Q.L. (2015). Tween 85 grafted PEIs enhanced delivery of antisense 2′-*O*-methyl phosphorothioate oligonucleotides *in vitro* and in dystrophic *mdx* mice. J. Mater. Chem. B Mater. Biol. Med. *3*, 5330–5340.

35. Wang, M., Wu, B., Tucker, J.D., Lu, P., and Lu, Q. (2015). Cationic polyelectrolyte-mediated delivery of antisense morpholino oligonucleotides for exon-skipping *in vitro* and in *mdx* mice. Int. J. Nanomedicine *10*, 5635–5646.

36. Juliano, R.L., Ming, X., and Nakagawa, O. (2012). Cellular uptake and intracellular trafficking of antisense and siRNA oligonucleotides. Bioconjug. Chem. *23*, 147–157.

37. Ming, X., Carver, K., and Wu, L. (2013). Albumin-based nanoconjugates for targeted delivery of therapeutic oligonucleotides. Biomaterials *34*, 7939–7949.

38. Sazani, P., Kang, S.H., Maier, M.A., Wei, C., Dillman, J., Summerton, J., Manoharan, M., and Kole, R. (2001). Nuclear antisense effects of neutral, anionic and cationic oligonucleotide analogs. Nucleic Acids Res. *29*, 3965–3974.

39. Hu, Y., Wu, B., Zillmer, A., Lu, P., Benrashid, E., Wang, M., Doran, T., Shaban, M., Wu, X., and Lu, Q.L. (2010). Guanine analogues enhance antisense oligonucleotide-induced exon skipping in dystrophin gene in vitro and in vivo. Mol. Ther. *18*, 812–818.

40. Juliano, R.L., Ming, X., Carver, K., and Laing, B. (2014). Cellular uptake and intracellular trafficking of oligonucleotides: implications for oligonucleotide pharmacology. Nucleic Acid Ther. *24*, 101–113.

41. Boussif, O., Lezoualc'h, F., Zanta, M.A., Mergny, M.D., Scherman, D., Demeneix, B., and Behr, J.P. (1995). A versatile vector for gene and oligonucleotide transfer into cells in culture and in vivo: polyethylenimine. Proc. Natl. Acad. Sci. USA *92*, 7297–7301.

42. Dominska, M., and Dykxhoorn, D.M. (2010). Breaking down the barriers: siRNA delivery and endosome escape. J. Cell Sci. *123*, 1183–1189.

43. Townsend, D., Yasuda, S., Li, S., Chamberlain, J.S., and Metzger, J.M. (2008). Emergent dilated cardiomyopathy caused by targeted repair of dystrophic skeletal muscle. Mol. Ther. *16*, 832–835.

44. Foster, K., Foster, H., and Dickson, J.G. (2006). Gene therapy progress and prospects: Duchenne muscular dystrophy. Gene Ther. *13*, 1677–1685.

45. Akhtar, S., and Benter, I.F. (2007). Nonviral delivery of synthetic siRNAs *in vivo*. J. Clin. Invest. *117*, 3623–3632.

46. Juliano, R., Bauman, J., Kang, H., and Ming, X. (2009). Biological barriers to therapy with antisense and siRNA oligonucleotides. Mol. Pharm. *6*, 686–695.

47. Whitehead, K.A., Langer, R., and Anderson, D.G. (2009). Knocking down barriers: advances in siRNA delivery. Nat. Rev. Drug Discov. *8*, 129–138.

48. Tamura, A., and Nagasaki, Y. (2010). Smart siRNA delivery systems based on polymeric nanoassemblies and nanoparticles. Nanomedicine (Lond.) *5*, 1089–1102.